Liên kết hydrogen không cổ điển C_{sp2}-H···O/Se/Te and O-H···Se/Te trong các hệ phức giữa acid formic acid và selenoformaldehyde, telluroformaldehydes

Tóm tắt

Trong nghiên cứu này, độ bền các phức cũng như các liên kết hydrogen và đặc trưng của chúng trong các hệ giữa acid formic với các dẫn xuất aldehyde được khảo sát một cách đầy đủ. Nhìn chung, độ bền của các phức được tăng cường đáng kể đối với các nhóm thế đẩy hoặc hút electron trong các dẫn xuất aldehyde. Các phức với dẫn xuất thế Se được tìm thấy bền hơn so với các phức Te. Các phức đối với sự thế halogen được đánh giá kém bền hơn so với các phức của dẫn xuất thế -CH_3 và –NH_2. Các kết quả thu được chỉ ra độ bền đáng kể của liên kết hydrogen O–H···Se/Te trong việc làm bền các phức so với C–H···O. Các kết quả tính toán cũng cho thấy rằng độ bền các liên kết hydrogen không cổ điển giảm theo thứ tự O–H···Se > O–H···Te ~ C–H···O > C–H···Se/Te. Sự chuyển dời xanh của liên kết hydrogen C–H···Se mạnh hơn so với C–H···Te. Phân tích NBO thấy rằng xu hướng chuyển dời xanh của tần số dao động liên kết C_{sp2}–H phụ thuộc chính vào sự giảm mật độ electron ở σ*(C_{sp2}–H) trong quá trình hình thành phức. Sự chuyển dời đỏ trong các liên kết hydrogen không cổ điển O-H···Se/Te được quyết định bởi sự tăng đáng kể mật độ electron tại σ*(O–H) so với sự tăng cường %s(O) trong quá trình tạo phức.

Từ khóa: *liên kết hydrogen không cổ điển O/C_{sp2}-H···O/Se/Te, Se/Te-aldehydes, acid formic.*

The C_{sp2}-H···O/Se/Te and O-H···Se/Te nonconventional hydrogen bonds in the systems of formic acid with selenoformaldehydes and telluroformaldehydes

ABSTRACT

In this study, a thorough investigation into the stability of complexes as well as the hydrogen bonds along with their characteristics in the systems between formic acid and chalcoaldehyde derivatives. Generally, the strength of complexes is enhanced irrespective of electron donating or withdrawing substitution in chalcoaldehyde derivatives. It is found that the complexes involving Se-substitution are slightly more stable than Te-one. The halogenated complexes are less stable than CH_3- and NH_2-substituted ones, in which the largest stability belongs to the complexes involving NH_2-substituted group. The obtained results show a dominant role of O–H···Se/Te compared to C–H···O in contributing to the stabilization of complexes. Calculated results indicate that the strength of nonconventional hydrogen bonds decreases in the order of O–H···Se > O–H··· Te ~ C–H···O > C–H···Se/Te. The larger blue shift of C-H bond in the complexes investigated is observed in C–H···O compared to C–H···Se/Te. The magnitude of blue shift is larger in the case of C–H···Se than in C–H···Te hydrogen bonds. NBO analysis shows that the blue-shifted stretching frequency of C_{sp2}–H depends mainly on a reduction of electron density at σ*(C_{sp2}–H) orbital. The redshift in O-H···Se/Te hydrogen bonds in these systems is determined by a considerable increase of electron density at σ*(O–H) orbitals overcoming a s-character enhancement of O site upon complexation.

Keywords: *O/C_{sp2}-H···O/Se/Te nonconventional hydrogen bonds, Se/Te-aldehydes, formic acid.*

1. INTRODUCTION

Hydrogen bonds play a crucial role in molecular information recognition, protein folding, structural rearrangement of nucleic acids, crystallization, polymerization, supramolecular chemistry, solvation, or organic synthesis.[1,2] Many investigations were performed to understand the characteristics of hydrogen bonds and their importance in the arrangement of molecules, surface phenomena,...[3-6] Noticeably, non-classical hydrogen bonds of the form C-H···O/N/X/π (X= F, Cl, Br) were detected in many systems including proteins, DNA, RNA, and material surfaces. Besides, the activation of C-H groups in intermediate structures is one of the issues of current interest in organic synthesis.[7,8] Experimental, Raman and theoretical findings of blue-shifted C-H bonds involved in hydrogen bonds have been reported, of which the most abundant is the C-H···O/N form.[9-17]

Several investigations focused on explaining the nature of blue-shifted hydrogen bonding, but none can be universally applied to other complex systems stabilized by hydrogen bonds.[9,16-20] Given the critical role of hydrogen bonds in biological systems, the strength and properties of classical hydrogen bonds O/S-H···O/S have been studied and reported by theoretical and experimental methods.[21,22] Many nonconventional hydrogen bonds have been discovered recently and play essential roles in proteins and catalysis. Indeed, the hydrogen bonds O/N-H···Se/Te were recently discovered experimentally.[23-24] Besides, the existence of H···Se hydrogen bonds in proteins and nucleobase pairs was determined by spectroscopic evidence.[25,26] However, systematic studies of the O-H···Se/Te hydrogen bond system to understand their strength and properties have not been reported. In addition, the influence of this O-H···Se/Te on the strength and characteristics of the C_{sp2}–H···Se/Te was not considered and evaluated in the literature.

In addition, the aldehydes, carboxylic acid, and their halogenated and amide derivatives are

commonly found in the biological structures and biologically active compounds. Theoretical studies indicated that the origin of stabilization in carboxylic acids and amide complexes is charge-delocalization.[2,27] The experimental and theoretical investigations into O-H redshift and C_{sp2}-H blueshift in the hydrogen bonds in formic acid, acetic acid, and acetaldehyde complexes were reported.[28-30] The strength and nature of blue- and red-shifting hydrogen bonds were examined in formamide, aldehydes, hydroxyl derivatives, and carboxylic acids.[31-33] More recently, the C_{sp2}-H blue shifting in the C_{sp2}–H···O hydrogen bonds have been reported for the complexes of aldehydes with formic acid, as well as the binary systems of aldehyde and carboxylic acids.[16,34,35]

Further, a theoretical study on the nature of hydrogen bonds in $NH_2CYH\cdots XH$ complexes with Y = O, S, Se, Te; X = F, HO, NH_2 was examined by quantum chemistry analyses.[36] Noticeably, the C_{sp2}-H···O/S/Se/Te hydrogen bonds were evaluated in the $XCHO\cdots nH_2Z$ and dimers of chalcogenoaldehyde derivatives systems.[37,38] However, the two hydrogen-bond systems between selenoformaldehyde or telluroformaldehyde and carboxylic acid and their derivatives have not yet been observed clearly. In addition, the effects of various X substituents relating to the strength of nonconventional hydrogen bonds and the shifts in C_{sp2}-H or O-H stretching frequency need to be addressed. Furthermore, the existence and role of various interactions following complexation, such as O-H···Se/Te and C_{sp2}-H···O/Se/Te, should be examined in the complexes of Se/Te derivatives to have insights into the nonconventional hydrogen bonds. In this work, the interaction complexes between aldehyde derivatives and formic acid are selected to have thorough insights into the effects of different substituent groups on the stability and characteristics of O-H···Se/Te, C_{sp2}-H···Se/Te nonconventional hydrogen bonds, and the complex strength.

2. COMPUTATIONAL METHODS

The optimized geometries for monomers and complexes are considered at the MP2/6-311++G(3df,2pd) level of theory with the correction of zero-point vibrational energies (ZPE). The interaction energy (ΔE^*) of each complex is calculated and corrected for basis set superposition errors (BSSE) at the CCSD(T)/6-311++G(3df,2pd)//MP2/6-311++G(3df,2pd) level. Particularly, ΔE^* is represented as the difference in total electronic energy between the complexes and the sum of XCHZ and HCOOH monomers given by the expression:

$$\mathbf{\Delta E^* = E_c - (E_{m1} + E_{m2})}.$$

Here, E_c is the energy of the optimized complexes including ZPE and BSSE corrections. E_{m1} and E_{m2} are energy values of the optimized monomers HCHZ and HCOOH, respectively, with the ZPE correction. Moreover, deprotonation enthalpy (DPE) is defined as the enthalpy change for the deprotonation reactions:

$XCHZ \rightarrow XCZ^- + H^+$ (1)

and $HCOOH \rightarrow HCOO^- + H^+$ (2)

and is considered as DPE of C-H and O-H bonds in both XCHZ and HCOOH monomers.

$DPE(C\text{-}H) = E^o(HCOO^-) - E^o(HCOOH) + TCE(HCOO^-) + TCE(H^+) - TCE(HCOOH)$, in which E^o and TCE values are electronic energy and thermal correction to the enthalpy of species, respectively.

In addition, proton affinity (PA) is defined as the enthalpy change for the protonation reaction:

$XCHZ + H^+ \rightarrow XCHZH^+$ (3)

and is considered PA at the Se and Te sites in XCHZ monomers.

$PA(Se/Te) = E^o(XCHZ) - E^o(XCHZH^+) + TCE(XCHZ) + TCE(H^+) - TCE(XCHZH^+)$.

These calculations are performed by the Gaussian 16 package.[39]

The Atoms-in-Molecules (AIM) analysis is observed at the MP2/6-311++G(3df,2pd) level through the AIMAll program.[40,41] The local electron energy density (H(r)) is computed from potential (V(r)) and kinetic (G(r)) terms by the equation:

$$\mathbf{H(r) = G(r) + V(r)}.$$

The individual energy of each hydrogen bond (E_{HB}) is estimated using the formula:

$$\mathbf{E_{HB} = 0.5V(r)}.$$[42]

Further, the natural bond orbital (NBO) analysis is examined by using NBO 5.G software at the range-separated hybrid functional ωB97X-D/6-311++G(3df,2pd) level.[43-45] Besides, Symmetry Adapted Perturbation Theory (SAPT) calculations based on the Psi4 program with the def2-TZVPD basis set are applied to unravel the different

contributions of energy components, including the electrostatic (E_{elec}), induction (E_{ind}), and dispersion (E_{disp}) to the stability of examined complexes.[46]

3. RESULTS AND DISCUSSION

3.1. Stable geometry and AIM analysis

The interaction of XCHZ with HCOOH induces 36 stable complexes, denoted by **XZ-n** (with X = H, F, Cl, Br, CH_3, NH_2; Z = Se, Te and n =1-3) with three geometries **XZ-n** displayed in Figure 1. The sp^2-hybridized carbon atom in XCHZ is labeled hereafter as C_{sp2}. Each complex contains a ring that is stabilized by two intermolecular contacts, including O–H···Se/Te and C_{sp2}–H···O in **XZ-1**, C–H···Se/Te and C_{sp2}–H···O in **XZ-2** and **XZ-3**. All H···O, H···Se and H···Te distances (Table S1) are in the range of 2.18–2.45 Å, 2.33–3.20 Å and 2.65–3.33 Å, respectively. These values are close to the sums of van der Waals radii of relevant atoms (being 2.72 Å for H···O, 3.00 Å for H···Se and 3.16 Å for H···Te). The presence of H···Se/Te and C_{sp2}–H···O/Se/Te nonconventional hydrogen bonds through the bonding critical points (BCPs, green points in Figure S1) is confirmed by the values of electron density, Laplacian, and H(r) at BCPs (Table S1).[41] Moreover, the C_{sp2}/O-H···Se/Te distances are also close to those in complexes between NH_2CHSe and NH_2CHTe, with $HF/H_2O/NH_3$.[47] The intermolecular contacts with the presence of chalcogen atoms (O, S, Se, Te) in hydrogen bonds were also reported in some studies.[16,34,36,48]

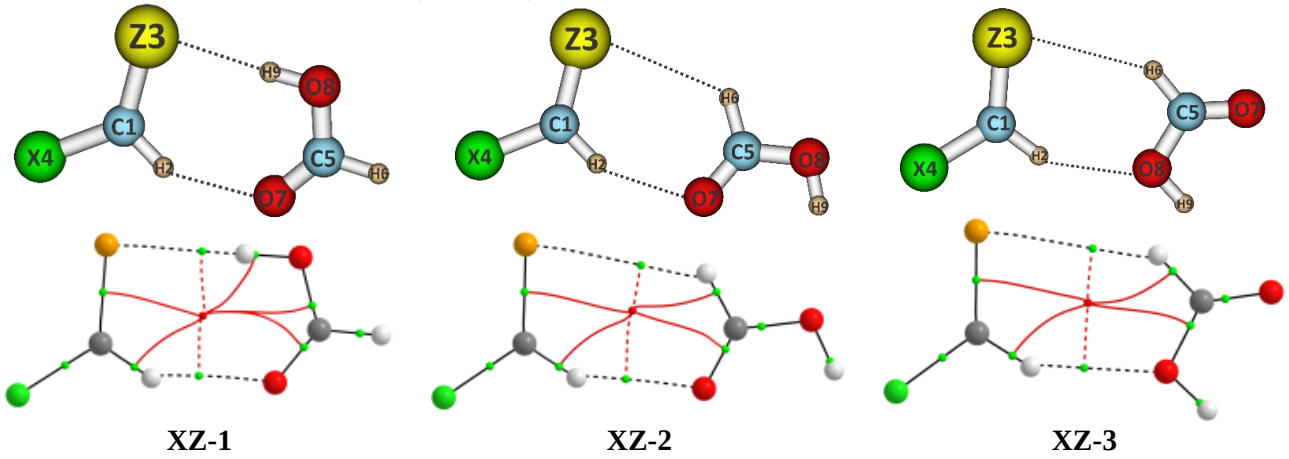

Figure 1: The stable structures and topological features of XCHZ and HCOOH complexes (X = H, F, Cl, Br, CH_3, NH_2 and Z = Se, Te)

In addition, the decreasing tendency of strength for hydrogen bonds is from O–H···Se to O–H···Te ~ C–H···O and then to C–H···Se/Te (Table S1). Indeed, the E_{HB} values indicate that the stability of C–H···O (-7.4 ÷ -15.6 kJ.mol^{-1}) is 2÷3 times as large as that of C–H···Se/Te (-3.3 ÷ -5.5 kJ.mol^{-1}). Similarly, the strength of O–H···Se (-16.8 ÷ -23.1 kJ.mol^{-1}) is 1.5 times as large as that of O–H···Te (-12.5 ÷ -13.8 kJ.mol^{-1}). Along with the results of individual hydrogen bond energies in literature by Khanh et al.[16], it is found that the hydrogen bond stability decreases in going from O–H···O >> O–H···S > O–H···Se > O–H···Te. These results are also supported by a previous investigation of hydrogen bonding complexes containing chalcogen atoms.[34] Besides, the second correlation of energy (E_{HB}) versus distances R(C-H···O/Se/Te) is obtained according to expression E_{HB} = -134.24 + 85.52R(C-H···O/Se/Te) -13.98R^2(C-H···O/Se/Te) (R^2 = 0.96) as given in Figure 2. However, a highly linear correlation of E_{HB} with respect to R(O-H···Se/Te is observed as expression E_{HB} = 29.205R(O-H···Se/Te) -78.638 (R^2 = 0.98). The results indicate that the shorter the intermolecular distance, the stronger the nonconventional hydrogen bond is, and vice versa.

As given in Table S1 of ESI, it can be suggested that the C–H···O hydrogen bonds play a main role in stabilizing **XZ-2** and **XZ-3** along with the addition of the C–H···Se/Te ones. Nevertheless, for **XZ-1** complexes, the C–H···O hydrogen bonds serve as a supplementary factor along with the substantial importance of the O–H···Se/Te ones in complex stabilization. To clarify the relationship between the strength of nonconventional hydrogen bonds and $r_{H\cdots O/Z}/\sum r_{vdW}$ ratio, the The $r_{H\cdots Z}/\sum r_{vdW}$ ratios are gathered and plotted in Table S1 and Figures S2, S3 of ESI. The results indicate a good agreement between the $r_{H\cdots Z}/\sum r_{vdW}$ ratio and E_{HB}

of nonconventional hydrogen bonds in investigated complexes. Indeed, the $r_{H\cdots Z}/\sum r_{vdW}$ ratios of C-H···O hydrogen bonds in the **XSe/Te-1** are smaller than those in **XSe/Te-2**, and **XSe/Te-3**. This result is consistent with the high stability of C-H···O hydrogen bonds in **XSe/Te-1** compared to **XSe/Te-2**, and **XSe/Te-3**. The $r_{H\cdots Z}/\sum r_{vdW}$ ratio of C-H···O increases in the order of NH_2 < Cl ~ Br < F < CH_3 < H substitutions, along with the decrease of C-H···O strength in the order: NH_2 > Cl ~ Br > F > CH_3 > H substituted derivatives. It is worth noted that the O-H···Se/Te hydrogen bonds are much more stronger than the C_{sp2}-H···Se/Te ones, which is proven by the much smaller $r_{H\cdots Z}/\sum r_{vdW}$ ratio of O-H···Se/Te that that of C_{sp2}-H···Se/Te hydrogen bonds. For **XZ-2** and **XZ-3**, the $r_{H\cdots Z}/\sum r_{vdW}$ ratios of C-H···Se/Te are larger than those of C-H···O, being in line with the weaker strength of the C-H···Se/Te than the C-H···O.

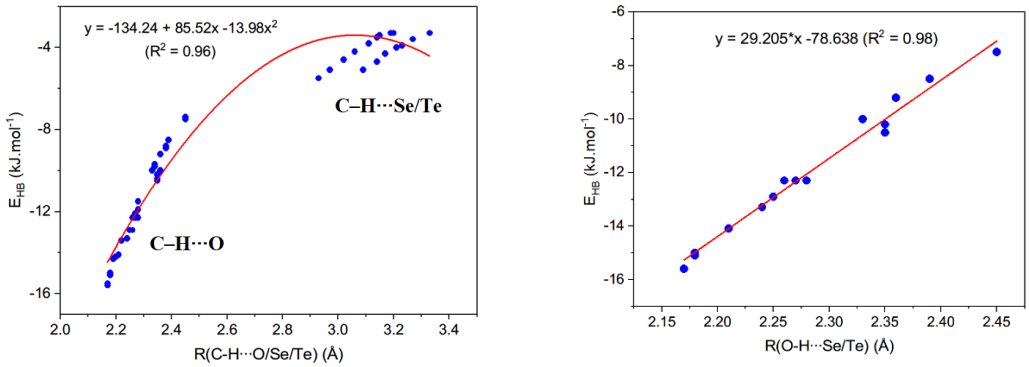

Figure 2: The relationships between E_{HB} and R(C/O-H···O/Se/Te) in the complexes

Table 1: Deprotonation enthalpies of C_{sp2}–H (DPE) and proton affinities at Z sites (PA) at the CCSD(T)/6-311++G(3df,2pd) (in kJ.mol^{-1})

Monomer	**HCHSe**	**FCHSe**	**ClCHSe**	**BrCHSe**	**CH_3CHSe**	**NH_2CHSe**
PA(Se)	775.0	737.9	766.3	773.0	811.7	860.0
DPE(C_{sp2}-H)	1623.6	1567.2	1551.7	1539.0	1620.7	1595.6
Monomer	**HCHTe**	**FCHTe**	**ClCHTe**	**BrCHTe**	**CH_3CHTe**	**NH_2CHTe**
PA(Te)	812.2	780.7	802.7	807.9	841.0	884.6
DPE(C_{sp2}-H)	1612.7	1561.0	1550.7	1540.8	1615.5	1582.3

Some characteristics of XCHZ monomers, including deprotonation enthalpies (DPE) and proton affinities (PA) are examined in Table 1. With the same Z in XCHZ, the strength of O-H···Z hydrogen bonds in **XZ-1** decreases in the order of NH_2 > CH_3 > H > F/Cl/Br substitutions (*cf.* Table S1), which are consistent with a decrease of gas-phase basicity (PA) at Se/Te site in XCHZ (*cf.* Table 1). However, a decrease in the strength of C-H···O hydrogen bonds in **XZ-1** is in the ordering NH_2 > F/Cl/Br > CH_3 > H substitutions, which differs from the trend of the polarity of C_{sp2}-H bond in the isolated XCHZ. As a result, the strength of **XZ-1** is mainly proposed by the presence of O-H···Z. Similarly, a decrease in gas-phase basicity at the Se/Te site in the sequence of NH_2 > CH_3 > H > F/Cl/Br derivatives causes a reduction of the strength of C-H···Z hydrogen bonds in **XZ-2, XZ-3** decrease in the same tendency. The strengthening trend of C-H···O hydrogen bonds in **XZ-2** and **XZ-3** is also suitable for an increase in the polarity of the C_{sp2}-H bond in XCHZ in the order of H < CH_3 < NH_2 < F/Cl/Br (cf. Table S1). With the identical X in XCHZ, the stronger strength of O–H···Se hydrogen bonds compared to O–H···Te ones is observed in **XZ-1**. However, for the same X in the isolated XCHZ, proton affinity at the Te site is larger than that at the Se one (cf. Table 1). Accordingly, these hydrogen bonds should be assigned by a larger electrostatic attraction of H and Se relative to H and Te.

3.2. Interaction energy and SAPT analysis

Interaction energies (ΔE*) of complexes, including both ZPE and BSSE correction at the CCSD(T)/6-311++G(3df,2pd)//MP2/6-311++G(3df,2pd) level are listed in Table 2, and their relationship is plotted in Figure 3. Generally, the ΔE* values in the range of -7.1 and -37.2 kJ.mol^{-1} indicate that the obtained complexes are quite stable, in which the **XZ-1** complexes are 2÷3 times as stable as **XZ-2** and **XZ-**

3 complexes. The considerable strength of **XZ-1** is suggested by the presence of O-H···Z hydrogen bond respective to the remaining nonconventional C-H···O/Z hydrogen bonds. The larger stability of **XZ-2** relative to **XZ-3** is due to the larger gas phase basicity of the O site of >C=O compared to that of the O site of –OH in formaldehyde acid. Both of them are stablized by the C-H···O/Z hydrogen bonds.

It is found that the most stable structures (**XZ-1**) of XCHZ···HCOOH in the present work have a comparable strength of XCHO···HCOOH complexes and are slightly larger than that of XCHS···HCOOH.[16] The **XZ-1** complexes are more stable than the binary complexes of small aldehydes and less stable than dimers of typical carboxylic acids. Indeed, the interaction energies of HCHO···HCHO, HCHO···HCHS, HCHS···HCHS are in turn -12.3, -11.7, -10.7 kJ.mol^{-1} at CCSD(T)-F12/heavy-aug-cc-pVTZ level of theory.[49] The complexes of HCHO···HCHO and CH_3CHO···CH_3CHO have interaction energies of -21.0 and -22.4 kJ.mol^{-1} at MP2/aug-cc-pVTZ.[50] The very large interaction energies of CH_3COOH···CH_3COOH and HCOOH···HCOOH at MP2/aug-cc-pVTZ are -60.7 kJ.mol^{-1} and -56.9 kJ.mol^{-1}.[51]

Table 2: Interaction energy corrected by both ZPE and BSSE (ΔE*, kJ.mol^{-1}) of the complexes RCHZ···HCOOH at CCSD(T)/6-311++G(3df,2pd)//MP2/6-311++G(3df,2pd)

Complex	△E*	**Complex**	△E*	**Complex**	△E*
HSe-1	-24.4	**HSe-2**	-10.7	**HSe-3**	-7.3
FSe-1	-23.9	**FSe-2**	-13.0	**FSe-3**	-8.1
ClSe-1	-24.9	**ClSe-2**	-12.9	**ClSe-3**	-8.4
BrSe-1	-24.7	**BrSe-2**	-12.9	**BrSe-3**	-8.6
CH_3Se-1	-28.4	**CH_3Se-2**	-12.3	**CH_3Se-3**	-8.9
NH_2Se-1	-37.2	**NH_2Se-2**	-16.6	**NH_2Se-3**	-11.7
HTe-1	-22.3	**HTe-2**	-10.2	**HTe-3**	-7.1
FTe-1	-22.9	**FTe-2**	-12.7	**FTe-3**	-8.1
ClTe-1	-23.6	**ClTe-2**	-12.7	**ClTe-3**	-8.3
BrTe-1	-23.5	**BrTe-2**	-12.6	**BrTe-3**	-8.5
CH_3Te-1	-25.8	**CH_3Te-2**	-11.8	**CH_3Te-3**	-8.4
NH_2Te-1	-34.7	**NH_2Te-2**	-16.6	**NH_2Te-3**	-11.4

It is noticeable that the interaction energy of **XSe–n** is *ca.* 0.1–2.6 kJ.mol$^{-1,}$ slightly more negative than that of **XTe–n**, about for the same X in XCHZ derivatives. This indicates a slightly lower strength of **XTe–n** as compared to **XSe–n,** which should be resulting from the stronger electrostatic force of Se and H atoms overcoming Te and H atoms.[34] Generally, the strength of **XZ-n** complexes is enhanced irrespective of electron donating or withdrawing X substitution (cf. Table 2 and Figure 3). For the alike Z, it is found that the halogenated complexes are less stable than CH_3- and NH_2-substituted ones. The largest stability belongs to the complexes **NH_2Z-n** with more negative values of 2.8-13.3 kJ.mol^{-1}. It can be suggested that O–H···Se/Te and C–H···O/Se/Te nonconventional hydrogen bonds play a significant role in contributing to the stability of **NH_2Z-n** compared to other complexes.

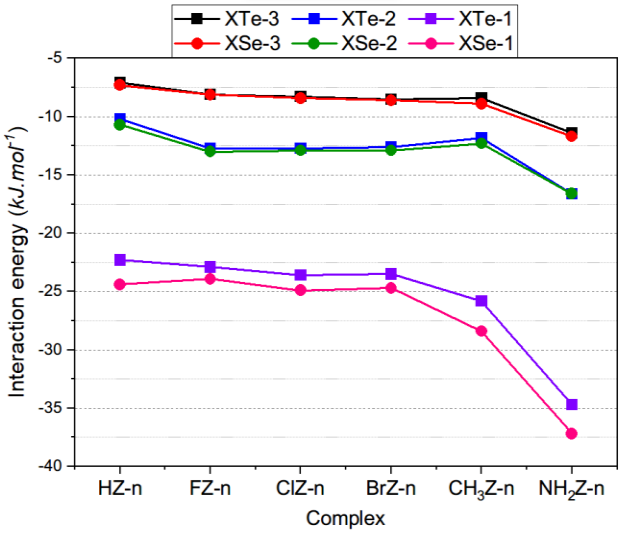

Figure 3: The relationship of the interaction energies and different X substitutions

As seen from Table 2, the interaction energy of complexes indeed increases in the substituting order: F < H < Br ~ Cl < CH_3 < NH_2 for **XSe-1** and H < F < Br ~ Cl < CH_3 < NH_2 for **XTe-1**. This result is suitable for the changing trend in the stability of O–H···Se/Te hydrogen bonds, affirming a main role of O–H···Se/Te along with an addition of C–H···O hydrogen bonds in stabilizing **XZ-1**. The energetic components based on the SAPT2+ approach are observed in Table S2. The calculated results imply the stability of complexes is mainly contributed by three terms, including electrostatic, dispersion, and induction, with contributing percentages of *ca.* 8-53%, 7-46% and 7-63%, respectively. The dominating role of electrostatic components contributing to the complex stability is also reported in the complexes of XCHO···HCOOH and XCHS···HCOOH.[16]

3.3. Characteristics of C_{sp2}-H···Se/Te and O-H···Se/Te nonconventional hydrogen bonds

The formation of C–H···Z, C–H···O and O–H···Z interactions in the complexes are further clarified by the change in lengths (Δr, mÅ) and the stretching frequencies (Δν, cm^{-1}) of O–H and C_{sp2}–H bond participating in the considered hydrogen bonds. The results at MP2/6-311++G(3df,2pd) are gathered in Table 3.

Considering the nonconventional hydrogen bonds of C–H···Se/Te, the C–H length in **XZ-2** and **XZ-3** decreases slightly in the range of 0.07–0.93 mÅ, accompanied by an increase in their stretching frequency of 1.9–14.8 cm^{-1} as compared to the corresponding values of isolated monomers. Therefore, these C–H···Se/Te contacts belong to blue-shifting hydrogen bonds. The larger blue shift of the C-H bond in the complexes investigated is observed in C–H···O compared to C–H···Se/Te and has a much smaller magnitude than that in the complexes of XCHO···HCOOH. It was found that all C-H···Se/Te nonconventional hydrogen bonds in dimers of RCHZ (R=H, F, Cl, Br or CH_3, Z= Se, Te) are red-shifted.[16] In the present work, a small C_{sp2}-H elongation of 0.10–0.52 mÅ along with a decrease in stretching frequency of 0.2–6.5 cm^{-1} is found in the case of **NH_2Se-3**, **BrTe-3**, **HTe-3**, **CH_3Te-3**, and **NH_2Te-3**, indicating red shifting hydrogen bonds. These values are quite close to a previous report of hydrogen bonded complexes.[37] The largest shortening of C-H bond length is observed for **FZ-2** and **FZ-3**, associated with the strongest electron-withdrawing group being F, whereas the smallest is observed in **NH_2Z-2** and **NH_2Z-3**. Besides, the blue shift of C–H6 bond in C5–H6···Z3 interaction in **XZ-2** and **XZ-3** decreases in the substituting order: F > Cl > Br > H > CH_3 > NH_2. This result is consistent with increased basicity at the Se/Te site in XCHZ (Table 1). The blue shift of the C_{sp2}-H bonds with the Z same is more strongly affected by electron-withdrawing groups (F, Cl, Br) than by electron-donating groups (CH_3, NH_2). The magnitude of the C5–H6 blue shift is larger for C–H···Se than for C–H···Te, which is in alignment with the increasing tendency of the proton affinity at Te relative to the Se site (cf. Table 1). Furthermore, the larger blueshift of the C–H bond in C–H···Z hydrogen bonds of **XZ-2** in comparison with that of **XZ-3** is

observed, which relates to the more crucial role of C–H···O hydrogen bond in **XZ-2** compared to that in **XZ-3**, toward the blue shift of C–H bonds.

Table 3: Changes in bond lengths (in mÅ) and their corresponding stretching frequencies (in cm^{-1}) at MP2/6-311++G(3df,2pd)

Complex	**HSe-1**	**FSe-1**	**ClSe-1**	**BrSe-1**	**CH_3Se-1**	**NH_2Se-1**	**HTe-1**	**FTe-1**	**ClTe-1**	**BrTe-1**	**CH_3Te-1**	**NH_2Te-1**
△r(C1H2)	0.42	0.76	1.54	1.77	-0.37	0.22	1.09	0.51	1.37	1.55	-0.08	0.69
△ν(C1H2)	8.4	3.8	-4.5	-6.8	18.9	8.1	0.3	7.2	-2.4	-4.6	14.3	1.6
△r(O8H9)	15.32	12.49	13.24	13.17	16.80	21.18	13.97	12.20	12.78	12.69	15.09	19.24
△ν(O8H9)	-326.2	-266.6	-284.0	-282.5	-355.5	-439.4	-299.5	-261.9	-274.6	-273.1	-322.1	-402.6
Complex	**HSe-2**	**FSe-2**	**ClSe-2**	**BrSe-2**	**CH_3Se-2**	**NH_2Se-2**	**HTe-2**	**FTe-2**	**ClTe-2**	**BrTe-2**	**CH_3Te-2**	**NH_2Te-2**
△r(C1H2)	0.17	0.21	0.76	0.92	-0.34	0.18	0.84	0.04	0.72	0.89	-0.20	0.53
△ν(C1H2)	7.8	7.8	3.0	1.2	15.6	6.9	-0.3	10.0	3.3	1.0	12.8	1.3
△r(C5H6)	-0.73	-0.93	-0.79	-0.76	-0.47	-0.30	-0.52	-0.78	-0.65	-0.60	-0.28	-0.07
△ν(C5H6)	11.8	14.8	13.0	12.5	8.7	6.5	7.3	11.2	9.5	8.8	4.3	1.9
Complex	**HSe-3**	**FSe-3**	**ClSe-3**	**BrSe-3**	**CH_3Se-3**	**NH_2Se-3**	**HTe-3**	**FTe-3**	**ClTe-3**	**BrTe-3**	**CH_3Te-3**	**NH_2Te-3**
△r(C1H2)	-0.07	-0.33	-0.17	-0.07	-0.48	-0.21	0.51	-0.36	-0.09	-0.04	-0.43	-0.05
△ν(C1H2)	10.1	13.4	13.6	12.6	16.7	12.5	3.5	13.6	12.5	11.8	15.2	9.9
△r(C5H6)	-0.07	-0.43	-0.20	-0.17	0.09	0.24	0.18	-0.16	0.06	0.10	0.38	0.52
△ν(C5H6)	3.2	8.5	5.4	4.9	1.1	-1.0	-1.8	3.3	0.3	-0.2	-4.4	-6.5

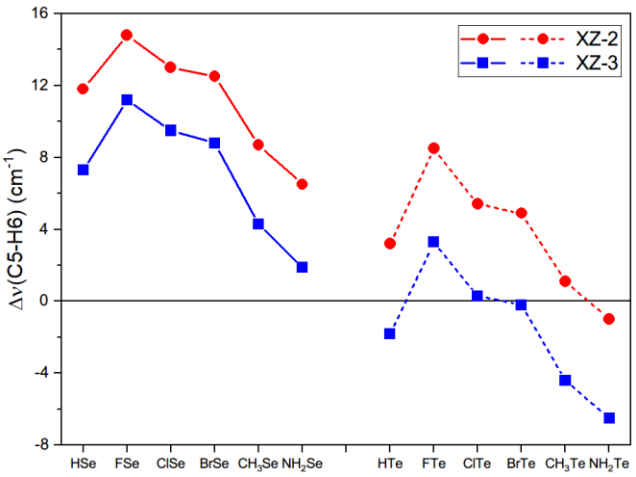

Figure 4: The relationship between the change in C-H stretching frequency and different X substitutions in **XZ-2** and **XZ-3**

For **XZ-3**, the C-H···O hydrogen bond displays a blue shift with a small contraction and an increase of C-H stretching frequency (Δr = -0.04 ÷ -0.48 *m*Å and Δν = 9.9 ÷16.7 cm^{-1}), except for a small elongation in **HTe-3**. Besides, the blue shift of the C-H bond observed in **XZ-2** is emphasized by a slight enhancement of its bond length and stretching frequency (except for **HTe-2,** with a slight redshift of C-H). A slight redshift is observed in **ClZ-1** and **BrZ-1**, while most **XZ-1** structures indicate a blue shifting of C–H···O hydrogen bonds. The redshift for hydrogen bonds in **ClZ-1** and **BrZ-1** is based on the high polarity of the C_{sp2}-H bonds in ClCHZ and BrCHZ monomers (Z = Se, Te).[16] As shown in Table 3, a C-H bond contraction and an increase in its stretching frequency in **XSe-n** are larger than those in **XTe-n**. This observation is

induced by the C-H strong polarity in **XCHTe** compared to **XCHSe**. Meanwhile, with the same Z in **XZ-3**, the larger blueshift in **CH_3Z-3** in comparison with **F/Cl/BrZ-3** comes from the smaller polarity of the C-H bond in **CH_3Z-3**. A very small blue shift of C_{Sp2}-H in C–H···O in XCHZ···HCOOH (Z=Se, Te) as compared to the considerable blue shift of that in XCHO···HCOOH (up to 100 cm^{-1}) was attained.[16] This shows the profound role of O-H···O relative to O-H···Se/Te in increasing the very considerable blue shift of the C_{sp2}-H bond. In other words, it implies a noticeable role of O related to S, Se and Te in the blue shifting of C–H···O hydrogen bonds.

On the other hand, for O–H···Se/Te hydrogen bonds in **XZ-1** form, the bond elongation of 12.5–21.2 mÅ for O–H···Se and 12.2–19.2 mÅ and O–H···Te is observed which is accompanied by a remarkable decrease of 266.6–439.4 cm^{-1} and 261.9–402.6 cm^{-1} in their stretching frequency, respectively (cf. Table 3). These changes show the redshift of O-H stretching frequencies involved in the O–H···Se/Te nonconventional hydrogen bonds. Particularly, with the same X in XCHZ, the redshift phenomenon in the O–H···Se hydrogen bonds is larger than the O–H···Te ones. In the case of the same Z, the redshift of O–H···Z hydrogen bonds is found in the increasing order of F/Cl/Br < H < CH_3 < NH_2 substitutions and agrees with the enhancement of proton affinity of chalcogen atom in the XCHZ (Table 1). The obtained result of the O-H red shift in the hydrogen bonds is similar to previous reports in complexes of chalcogen derivatives and formic acid.[16,34]

3.4. NBO analysis

In order to determine the strength and characteristics of intermolecular interactions and complexes investigated, the NBO analysis is carried out at ωB97X-D/6-311++G(3df,2pd), as presented in Table 4. The positive values of electron density transfer (EDT) for most complexes (0.0003–0.0587 e) imply that the electron density is transferred mainly from XCHZ to HCOOH. This tendency is caused by the large energy of electron transfer n(Z3)→σ*(C5–H6) (7.02-20.57 $kJ.mol^{-1}$) and n(Z3)→σ*(O8–H9) (65.42-109.35 $kJ.mol^{-1}$) in comparison to n(O7/O8)→σ*(C1–H2) (2.88-14.59 $kJ.mol^{-1}$), except for **FSe-2**, **ClSe-2** and **BrSe-2** with the negative values of EDT. Hence, the n(Z3)→σ*(C5–H6) and n(Z3)→σ*(O8–H9) electron density transfers play a dominant role in stabilizing most complexes as compared to the n(O7/O8)→σ*(C–H) transfers. A larger role of n(O7)→σ*(C1–H2) (10.58-11.41 $kJ.mol^{-1}$) related to n(Z3)→σ*(C5–H6) (7.02-7.48 $kJ.mol^{-1}$) is found in **FSe-2**, **ClSe-2** and **BrSe-2** (cf. Table 4). This result should be due to the stronger polarity of the C-H bond in XCHSe (with X=F, Cl, Br), leading to the larger ability of electron acceptance of σ*(C1–H2) orbital.

The very large E_{inter} values of n(Z3)→σ*(O8–H9) in **XZ-1** compared to n(Z3)→σ*(C5–H6) in **XZ-2** and **XZ-3** indicate that the much stronger electron density transfers from lone pair of electrons from Z3 to σ*(O8–H9) orbitals are much stronger than from Z3 to σ*(C5–H6) ones. Moreover, E_{inter}[n(O7/O8)→σ*(C1–H2)] is higher for **XZ-1** than **XZ-2** and **XZ-3**, implying a stronger electron density transfer in **XZ-1**. These obtained results of E_{inter} are consistent with the trend in the stability of hydrogen bonds as analyzed in the AIM part above.

For changing X in XCHZ, E_{inter}[n(Z3)→σ*(C5–H6)] in **XZ-2**, **XZ-3** and E_{inter}[n(Z3) → σ*(O8–H9)] in **XZ-1** increase in the order of F/Cl/Br < H < CH_3 < NH_2 substituents, suitable for the increasing trend of the proton affinity at Z3 site (Table 1). In other words, the intermolecular charge density transfers from XCHZ to HCOOH are raised by the presence of CH_3 and NH_2 groups and are diminished by halogen substituents. It is noted that the increase in values of E_{inter}[n(O7/O8)→σ*(C1–H2)] is attained by the substitution of electron-donating or electron-withdrawing groups.

Table 4: Electron density transfer (EDT), hyperconjugation interaction energies (E_{inter}, in $kJ.mol^{-1}$), and changes of electron density (△σ*, in electron) and s-character percentage of atom involving hydrogen bond (△%s, in %)

Complex	HSe-1	FSe-1	ClSe-1	BrSe-1	CH_3Se-1	NH_2Se-1	HTe-1	FTe-1	ClTe-1	BrTe-1	CH_3Te-1	NH_2Te-1
EDT	0.051	0.036	0.039	0.038	0.052	0.059	0.050	0.039	0.041	0.040	0.050	0.056
E_{inter}[n(O7)→σ*(C1-H2)]	9.28	12.54	13.21	12.25	9.91	14.59	7.36	9.99	10.83	10.03	8.23	13.54
E_{inter}[n(Z3)→σ*(O8-H9)]	84.06	68.05	70.77	68.76	90.54	109.35	75.32	65.42	67.51	66.00	77.16	95.35
△σ*(C1-H2)	-0.002	-0.002	-0.002	-0.002	-0.002	-0.002	-0.001	-0.001	-0.001	-0.001	-0.001	-0.001

△%s(C1)	1.51	1.68	1.71	1.71	1.52	1.74	1.43	1.66	1.72	1.74	1.43	1.71
△σ*(O8-H9)	0.052	0.042	0.045	0.045	0.055	0.064	0.051	0.044	0.046	0.046	0.053	0.061
△%s(O8)	3.37	2.97	3.07	3.03	3.57	4.07	3.05	2.78	2.85	2.83	3.23	3.70
Complex	**HSe-2**	**FSe-2**	**ClSe-2**	**BrSe-2**	**CH_3Se-2**	**NH_2Se-2**	**HTe-2**	**FTe-2**	**ClTe-2**	**BrTe-2**	**CH_3Te-2**	**NH_2Te-2**
EDT	0.003	-0.002	-0.002	-0.002	0.003	0.003	0.005	0.001	0.001	0.001	0.004	0.004
E_{inter}[n(O7)→σ*(C1-H2)]	7.61	10.58	11.41	10.78	7.61	10.45	6.65	8.69	9.78	9.32	6.98	10.7
E_{inter}[n(Z3)→σ*(C5-H6)]	9.41	7.02	7.48	7.48	11.37	14.59	10.91	9.03	9.28	9.28	12.79	16.39
△σ*(C1-H2)	-0.001	-0.002	-0.002	-0.002	-0.002	-0.001	-0.001	-0.001	-0.001	-0.001	-0.001	-0.001
△%s(C1)	1.13	1.3	1.44	1.5	1.1	1.21	1.12	1.31	1.46	1.52	1.11	1.26
△σ*(C5-H6)	0.001	-0.001	-0.001	-0.001	0.001	-0.001	0.003	0.002	0.002	0.002	0.003	0.002
△%s(C5)	0.50	0.38	0.39	0.38	0.61	0.86	0.45	0.37	0.37	0.37	0.55	0.80
Complex	**HSe-3**	**FSe-3**	**ClSe-3**	**BrSe-3**	**CH_3Se-3**	**NH_2Se-3**	**HTe-3**	**FTe-3**	**ClTe-3**	**BrTe-3**	**CH_3Te-3**	**NH_2Te-3**
EDT	0.007	0.002	0.002	0.002	0.006	0.007	0.009	0.005	0.005	0.005	0.008	0.010
E_{inter}[n(O8)→σ*(C1-H2)]	3.51	5.68	5.89	5.39	3.64	4.85	2.88	4.39	4.93	4.51	2.97	4.47
E_{inter}[n(Z3)→σ*(C5-H6)]	12.5	9.45	10.03	9.82	14.3	18.22	14.71	12.46	12.79	12.58	16.59	20.57
△σ*(C1-H2)	-0.001	-0.001	-0.001	-0.001	-0.001	-0.001	-0.001	-0.001	-0.001	-0.001	-0.001	0.001
△%s(C1)	0.72	0.84	0.94	0.97	0.68	0.76	0.72	0.85	0.96	1.00	0.68	0.80
△σ*(C5-H6)	0.003	0.001	0.002	0.002	0.003	0.002	0.005	0.004	0.004	0.004	0.005	0.005
△%s(C5)	0.72	0.64	0.64	0.63	0.83	1.15	0.66	0.62	0.61	0.60	0.75	1.09

(EDT, E_{inter} at ωB97X-D/6-311++G(3df,2pd); △σ, △%s at MP2/6-311++G(3df,2pd))*

The C1-H2 blueshift in C1–H2···O7/O8 is caused by a small decrease of electron density at σ*(C1–H2) orbital from 0.001e to 0.002e (excepting for a very slight increase of σ*(C_{sp2}–H) occupation in **NH_2Te-3**). Generally, the blueshift of C5-H6 in the complexes is emphasized by a slight increase in electron density at σ*(C5–H6) from -0.001e to 0.005e. The O8-H9 redshift is induced by a large increase in electron density at σ*(O8-H9) orbital from 0.042e to 0.064e. The larger blueshift of C5-H6 is observed in **XSe-n** compared to **XTe-n.** Indeed, the electron density of the σ*(C5–H6) orbital gets a larger increase when Se is replaced by Te, and s–character percentage of C5 is smaller for C5–H6···Te3 than C5–H6···Se3. The larger blueshift of C5-H6···Se3 bonds, which relates directly to the smaller values of Δσ*(C5-H6), is found in **XZ-2** in comparison to **XZ-3**. Moreover, the substitution of the H atom in HCHZ by electron-donating groups (CH_3, NH_2) leads to an enhancement of C_{sp2}–H stretching frequency involving C_{sp2}–H···Z hydrogen bonds. At the same time, the corresponding diminishment is caused by the presence of electron-withdrawing groups (F, Cl, Br). Consequently, it can be underlined that the larger contraction of the C_{sp2}-H bond and its stretching frequency blueshift is identified by a decrease in the population of electron density at σ*(C5–H6) orbitals and an increase in the percentage of s-character of C_{sp2} atom. This observation is similar to results obtained in complexes of aldehydes and carboxylic acids.[16,34,37]

For C1-H2···O7/O8 hydrogen bonds, the stronger blueshift of C1-H2 in **XSe-n** compared to that in **XTe-n** relates to a more significant decrease of electron density in σ*(C1–H2) orbital. The larger redshift phenomenon in the O8–H9···Se hydrogen bonds compared to the O8–H9···Te ones (cf. Table 4) arises from a significant enhancement in occupation of σ*(O8–H9) orbital. Besides, the increase in electron density of σ*(O8–H9) orbital and s-character percentage of the O8 site is smaller for halogenated derivatives than for CH_3 and NH_2 substitutions. It can be suggested that the increasing occupation of σ*(O8–H9) orbital is the main factor in determining red-shifting hydrogen bonds in all examined complexes.

4. CONCLUSION

Thirty-six stable structures of XCHZ-HCOOH complexes with three various geometric structures (X = H, F, Cl, Br, CH_3, NH_2; Z = Se, Te) are

located on the potential energy surfaces. The binding energy of C_{sp2}–H···Se/Te bonds (from -3.3 to -5.5 kJ.mol^{-1}) is smaller than C_{sp2}–H···O and O–H···Te nonconventional hydrogen bonds (from -7.4 to -15.6 kJ.mol^{-1}) and is *ca*. half of O–H···Se ones (from -12.4 to -23.1 kJ.mol^{-1}). Following complexation, the O–H···Se/Te bond strength is determined by proton affinity at the Z atom of XCHZ, while the polarity of C_{sp2}–H covalent bonds in XCHZ plays a decisive role in stabilizing C_{sp2}–H···O/Se/Te hydrogen bonds. The existence and stability of nonconventional hydrogen bonds in the investigated systems are clarified by AIM and NBO analyses. With the same X, the C_{sp2}–H···O/Se/Te hydrogen bonds in **XSe-2** and **XTe-2** are more stable than in **XSe-3** and **XTe-3**. The significantly larger stability of O–H···Se hydrogen bonds compared to C_{sp2}–H···O/Se/Te causes a larger strength of **XSe-1** and **XTe-1,** in which **XZ-1** is twice more stable than **XZ-2** and **XZ-3**. With the same Z, the stability of complexes experiences an enhancement upon substituting one H in XCHZ by a CH_3 group, an NH_2 group, or a halogen atom (F, Cl, Br). Remarkably, it is found that the electron-donating groups make the complex more stable than the electron-withdrawing groups. Furthermore, the results from NBO analysis illustrate that all the O–H···Se/Te hydrogen bonds are redshifted, resulting from a noticeable electron density increase of σ*(O–H) orbital following complexation. The C_{sp2}–H bond in the C–H···O/Se/Te is transferred from the blueshift to redshift in ordering O and Se and then to Te substitution. This result is suggested by a slight decrease of electron density at σ*(C_{sp2}–H) orbital and a rise in s-character percentage of C in C_{sp2}–H bonds upon complexation.

REFERENCES

1. G. A. Jeffrey, W. Saenger. *Hydrogen bonding in biological structures*, Springer-Verlag Berlin Heidelberg, 1991.
2. S. J. Grabowski. *Hydrogen bonding – New insights, In J. Leszczynski (Ed.), Series challenges and advances in computational chemistry and physics*, New York, NY: Springer, 2006.
3. J. D. Olivier, F. Marc, C. Enric. Activation of C−H···halogen (Cl, Br, and I) hydrogen bonds at the organic/inorganic interface in fluorinated tetrathiafulvalenes salts, *Chem. Eur. J.*, **2001**, *7(12)*, 2635.
4. J. J. J. Dom, B. Michielsen, B. U. W. Maes, W. A. Herrebout, B. J. van der Veken. The C–H···π interaction in the halothane/ethene complex: a cryosolution infrared and Raman study, *Chem. Phys. Lett.*, **2009**, *469*, 85.
5. J. M. Hermida-Ramon, A. M. Grana. Blue-shifting hydrogen bond in the benzene–benzene and benzene–naphthalene complexes, *J. Comput. Chem.*, **2007**, *28*, 540.
6. C. D. Keefe, M. Isenor. Ab initio study of the interaction of CHX_3 (X = H, F, Cl, or Br) with benzene and hexafluorobenzene, *J. Phys. Chem. A*, **2008**, *112*, 3127.
7. L. S. Sremaniak, J. L. Whitten, M. J. Truitt, J. L. White. Weak hydrogen bonding can initiate alkane C−H bond activation in acidic zeolites, *J. Phys. Chem. B*, **2006**, *110(42)*, 20762.
8. R. E. Plata, D. E. Hill, B. E. Haines, D. G. Musaev, L. Chu, D. P. Hickey, M. S. Sigman, J-Q. Yu. Blackmond_D. G., A Role for Pd(IV) in catalytic enantioselective C–H functionalization with monoprotected amino acid ligands under mild conditions, *J. Am. Chem. Soc.*, **2017**, *139* (27), 9238.
9. P. R. Shirhatti, S. Wategaonkar. Blue shifted hydrogen bond in 3-methylindole·CHX_3 complexes (X = Cl, F), *Phys. Chem. Chem. Phys.*, **2010**, *12*, 6650.
10. P. R. Shirhatti, D. K. Maity, S. Wategaonkar. C–H···Y hydrogen bonds in the complexes of p-cresol and p-cyanophenol with fluoroform and chloroform, *J. Phys. Chem. A*, **2013**, *117*, 2307.
11. W. A. Herrebout, S. M. Melikova, S. N. Delanoye, K. S. Rutkowski, D. N. Shchepkin, B. J. van der Veken. A cryosolution infrared study of the complexes of fluoroform with ammonia and pyridine: evidence for a C−H···N pseudo blueshifting hydrogen bond, *J. Phys. Chem. A*, **2005**, *109*, 3038.
12. B. G. Oliveira, R. C. M. U. de Araújo, M. N. Ramos. A theoretical study of blueshifting hydrogen bonds in π weakly bound complexes, *J. Mol. Struct. (Theochem.)*, **2009**, *908*, 79.
13. R. Gopi, N. Ramanathan, K. Sundararajan. Experimental evidence for blue-shifted hydrogen bonding in the fluoroform–hydrogen chloride complex: a matrix-isolation infrared and ab initio study, *J. Phys. Chem. A*, **2014**, *118*, 5529.
14. B. Behera, P. K. Das. Blue-shifted hydrogen bonding in the gas phase CH/D_3CN···$HCCl_3$ complexes, *J. Phys. Chem. A*, **2019**, *123*, 1830.
15. I. S. Sosulin, E. S. Shiryeva, D. A. Tyurin, V. I. Feldman. Matrix isolation and ab initio study on the CHF_3···CO complex, *J. Phys. Chem. A*, **2018**, *122*, 4042.
16. N. T. Trung, P. N. Khanh, A. J. P. Carvalho, M. T. Nguyen. Remarkable shifts of C_{sp2}-H and O-H stretching frequencies and stability of complexes of formic acid with formaldehydes and thioformaldehydes, *J. Comput. Chem.*, **2019**, *40*, 1387.

17. R. Gopi, N. Ramanathan, N. Sundararajan. Blueshift of the C-H stretching vibration in CHF_3-H_2O complex: matrix isolation infrared spectroscopy and ab initio computations, *Chem. Phys.*, **2016**, *476*, 36.
18. Y. Mao, M. Head-Gordon. Probing blue-shifting hydrogen bonds with adiabatic energy decomposition analysis, *J. Phys. Chem. Lett.*, **2019**, *10*, 3899.
19. C. Wang, D. Danovich, S. Shaik, Y. Mo. A unified theory for the blue- and red-shifting phenomena in hydrogen and halogen bonds, *J. Chem. Theory Comput.*, **2017**, *13*, 1626.
20. Y. Mo, C. Wang, L. Guan, B. Braïda, P. C. Hiberty, W. Wu. On the nature of blueshifting hydrogen bonds, *Chem. – Eur. J.*, **2014**, *20*, 8444.
21. B. J. Mintz, J. M. Parks. Benchmark interaction energies for biologically relevant noncovalent complexes containing divalent sulfur, *J. Phys. Chem. A*, **2012**, *116*, 1086.
22. S. Sarkar, M. B. Bandyopadhyay. Cooperative nature of the sulfur centered hydrogen bond: investigation of $(H_2S)_n$ (n = 2–4) clusters using an affordable yet accurate level of theory, *Phys. Chem. Chem. Phys.*, **2019**, *21*, 25439.
23. K. K. Mishra, S. K. Singh, P. Ghosh, D. Ghosh, A. Das. The nature of selenium hydrogen bonding: gas phase spectroscopy and quantum chemistry calculations, *Phys. Chem. Chem. Phys.*, **2017**, *19*, 24179.
24. K. K. Mishra, S. K. Singh, K. Kumar, G. Singh, B. Sarkar, M. S. Madhusudhan, A. Das. Water-mediated selenium hydrogen-bonding in proteins: pdb analysis and gas-phase spectroscopy of model complexes, *J. Phys. Chem. A*, **2019**, *123*, 5995.
25. V. R. Mundlapati, D. K. Sahoo, S. Ghosh, U. K. Purame, S. Pandey, R. Acharya, N. Pal, P. Tiwari, H. S. Biswal. Spectroscopic evidences for strong hydrogen bonds with selenomethionine in proteins, *J. Phys. Chem. Lett.*, **2017**, *8*, 794.
26. J. Salon, J. Sheng, J. S. Jiang, G. X. Chen, J. Caton-Williams and Z. Huang. Oxygen replacement with selenium at the thymidine 4-position for the Se base pairing and crystal structure studies, *J. Am. Chem. Soc.*, **2007**, *129*, 4862.
27. R. W. Gora, S. J. Grabowski, J. Leszczynski. Dimers of formic acid, acetic acid, formamide and pyrrole-2 carboxylic acid: an ab initio study, *J. Phys. Chem. A*, **2005**, 109, 6397.
28. R. W. Góra, M. Maj and S. J. Grabowski. Resonance-assisted hydrogen bonds revisited. Resonance stabilization vs. charge delocalization, *Phys. Chem. Chem. Phys.*, **2013**, *15*, 2514.
29. K. C. Asit and Z.-H. Therese. Theoretical Investigation of the Cooperativity in $CH_3CHO\cdots 2H_2O$, $CH_2FCHO\cdots 2H_2O$, and $CH_3CFO\cdots 2H_2O$ Systems, *Journal of Atomic, Molecular, and Optical Physics*, **2012**, *0*, 1.
30. K. Tabayashi, O. Takahashi, H. Namatame, M. Taniguchi. Substituent R-effects on the core–electron excitation spectra of hydrogen-bonded carboxylic-acid (R–COOH) clusters: Comparison between acetic-acid and formic-acid clusters, *Chem. Phys. Lett.*, **2013**, *557*, 1.
31. T. S. Thakur, M. T. Kirchner, D. Bläser, R. Boese, G. R. Desiraju. Nature and strength of C–H···O interactions involving formyl hydrogen atoms: computational and experimental studies of small aldehydes, *Phys. Chem. Chem. Phys.*, **2011**, *13*, 14076.
32. K. Damanjit, K. Rajinder. Theoretical Characterization of Hydrogen Bonding Interactions between RCHO (R = H, CN, CF_3, OCH_3, NH_2) and HOR′ (R′= H, Cl, CH_3, NH_2, C(O)H, C_6H_5), *J. Chem. Sci.*, **2015**, *127*, 1299.
33. Q. Zhang, L. Du. Hydrogen bonding in the carboxylic acid–aldehyde complexes, *Comput. Theor. Chem.*, **2016**, *1078*, 123.
34. N. T. T. Cuc, N. T. An, V. T. Ngan, N. T. Trung. Importance of water and intramolecular interaction governs substantial blue shift of C_{sp2}–H stretching frequency in complexes between chalcogenoaldehydes and water, *RSC Adv.*, **2022**, *12*, 1998.
35. N. T. An, V. T. Ngan, N. T. Trung. Profound importance of the conventional O–H O hydrogen bond versus a considerable blue shift of the C_{sp2}–H bond in complexes of substituted carbonyls and carboxyl, *Phys. Chem. Chem. Phys.*, **2024**, *26*, 22775.
36. Y. Yang, W. T. Zhang. Theoretical study on blue-shifted hydrogen bonds in CH_3CHO dimers, *Acta Chim. Sin.*, **2009**, *67*, 599.
37. N. T. T. Cuc, P. D. Cam-Tu, N. T. A. Nhung, M. T. Nguyen, N. T. Trung, V. T. Ngan. Theoretical Aspects of Nonconventional Hydrogen Bonds in the Complexes of Aldehydes and Hydrogen Chalcogenides, *J. Phys. Chem. A*, **2021**, *125(48)*, 10291.
38. L. T. T. Quyen, B. N.Tung, P. N. Thach, N. N. Tri and N. T. Trung. Characteristics of nonconventional hydrogen bonds and stability of dimers of chalcogenoaldehyde derivatives: a noticeable role of oxygen compared to other chalcogens, *RSC Adv.*, **2024**, *14*, 14114.
39. M. J. Frisch, G. W. Trucks and H. B. Schlegel, et al. *Gaussian 16 Rev. A. 03*, Gaussian Inc., Wallingford CT, 2016.
40. T. A. Keith. *AIMAll (Version 19.10.12)*, TK Gristmill Software, Overland Park KS, USA, 2019.
41. P. L. Popelier. *Atoms in Molecules: An Introduction*, Prentice Hall, London, 2000.
42. I. Mata, I. Alkorta, E. Espinosa, E. Molins. Relationships between interaction energy, intermolecular distance and electron density properties in hydrogen bonded complexes under

external electric fields, *Chem. Phys. Lett.*, **2011**, *507*, 185.
43. E. D. Glendening, J. K. Baderhoop, A. E. Read, J. E. Carpenter, J. A. Bohmann and F. Weinhold. *GenNBO 5.G*, Theoretical Chemistry Institute, University of Wisconsin Madison, WI, 2001.
44. F. Weinhold and C. R. Landis. Natural Bond Orbitals and Extensions of Localized Bonding Concepts, *Chem. Educ. Res. Pract.*, **2001**, *2*, 91.
45. J. D. Chai and M. Head-Gordon. Long-range corrected hybrid density functionals with damped atom–atom dispersion corrections, *Phys. Chem. Chem. Phys.*, **2008**, *10*, 6615.
46. J. M. Turney, A. C. Simmonett, R. M. Parrish, E. G. Hohenstein, F. A. Evangelista, J. T. Fermann, B. J. Mintz, L. A. Burns, J. J. Wilke, M. L. Abrams, N. J. Russ, M. L. Leininger, C. L. Janssen, E. T. Seidl, Q. D. Allen, H. F. Schaefer, R. A. King, E. F. Valeev, C. D. Sherrill, T. D. Crawford. Psi4: an open-source ab initio electronic structure program, *WIREs. Comput. Mol. Sci.*, **2012**, *2(4)*, 556.
47. S. Bedoura, H.-W. Xi, K. H. Lim. Hydrogen bond nature in formamide ($CYHNH_2\cdots XH$; Y= O, S, Se, Te; X = F, HO, NH_2) complexes at their ground and low-lying excited states, *J. Phys. Org. Chem.*, **2014**, *27(3)*, 226.
48. N. T. An, N. T. Duong, N. N. Tri, and N. T. Trung. Role of O–H···O/S conventional hydrogen bonds in considerable C_{sp2}–H blueshift in the binary systems of acetaldehyde and thioacetaldehyde with substituted carboxylic and thiocarboxylic acids, *RSC Adv.*, **2022**, *12(54)*, 35309.
49. E. V. Dornshuld, C. M. Holy, G. S. Tschumper. Homogeneous and heterogeneous noncovalent dimers of formaldehyde and thioformaldehyde: structures, energetics, and vibrational frequencies, *J. Phys. Chem. A*, **2014**, *118*, 3376.
50. I. V. Alabugin, S. Bresch, M. Manoharan. Hybridization Trends for Main Group Elements and Expanding the Bent's Rule Beyond Carbon: More than Electronegativity, *J. Phys. Chem. A*, **2014**, *118*, 3663.
51. G. A. Dolgonos. Which isomeric form of formaldehyde dimer is the most stable – a high-level coupled-cluster study, *Chem. Phys. Lett.*, **2013**, *585*, 37.